Biochemical Pharmacology 175 (2020) 113922

Contents lists available at ScienceDirect

Biochemical Pharmacology

journal homepage: www.elsevier.com/locate/biochempharm

HIF-1 stabilization exerts anticancer effects in breast cancer cells *in vitro* and *in vivo*

Neli Kachamakova-Trojanowska[a,b], Paulina Podkalicka[a], Tomasz Bogacz[a], Szymon Barwacz[a], Alicja Józkowicz[a], Józef Dulak[a], Agnieszka Łoboda[a,*]

[a] Department of Medical Biotechnology, Faculty of Biochemistry, Biophysics and Biotechnology, Jagiellonian University, Gronostajowa 7, 30-387 Kraków, Poland
[b] Malopolska Centre of Biotechnology, Jagiellonian University, Gronostajowa 7a, 30-387 Kraków, Poland

ARTICLE INFO

Keywords:
Tumorigenesis
Prolyl hydroxylase inhibitor
HIF-1
Breast cancer
Angiogenesis

ABSTRACT

Tumor hypoxia and high activity of hypoxia-inducible factor-1 (HIF-1) correlate with adverse disease outcomes, malignancy, resistance to therapy and metastasis. Nonetheless, recent studies indicate that under certain circumstances, HIF-1 stabilization may exert protective effects and even decrease tumor cell aggressiveness.

This study aimed to characterize the potential anticancer effect of molidustat (BAY 85-3934), the prolyl hydroxylase (PHD) inhibitor and HIF-1 stabilizator. We confirmed that molidustat stabilizes HIF-1α and induces the expression of vascular endothelial growth factor (VEGF) in MDA-MB-231 breast cancer cells, to a similar or even greater extent than hypoxia. Interestingly, decreased cell survival and colony formation capabilities, together with S/G2 cell cycle arrest, were observed after treatment with PHD inhibitor. Importantly, molidustat enhanced the effectiveness of the chemotherapeutic drug, gemcitabine, on cancer cells. Finally, the xenograft model revealed decreased tumor growth *in vivo* after molidustat treatment. Both *in vitro* and *in vivo* analysis showed no differences in the angiogenic potential of endothelial cells treated with tumor-conditioned media or vascularization of the MDA-MB-231 xenografts, respectively.

In summary, molidustat treatment exhibits an inhibitory effect on breast cancer cell survival, self-renewal capacity and potentiates the efficacy of chemotherapeutic gemcitabine.

1. Introduction

Breast cancer is a global health concern and is currently the most common tumor in the world. According to the WHO reports, ~ 2 million women are diagnosed with breast cancer each year. Although evaluation of BRCA1/2 mutations (as well as mutations in other oncogenes and suppressor genes) is used to better define the prognosis and treatment of breast cancer-affected patients, as this type of tumor displays a large degree of inter- and intratumoral heterogeneity, there is a huge difference in the survival rates worldwide [1–3]. Therefore, understanding the conditions affecting tumor growth and heterogeneity may help discover new therapies and make the disease preventable.

One of the conditions highly related to tumorigenesis is hypoxia. The activity of hypoxia-inducible factor-1 (HIF-1), the transcription factor stabilized in response to low oxygen concentrations, is one of the main regulators of genes involved in multiple pathways, including metabolism, angiogenesis and cell cycle regulation [4]. All those processes are also indispensably important for tumor growth and metastasis. Moreover, the strong association of HIF-1 activation with cancer development, including breast cancer [5], has been shown. From many HIF-1 target genes, those encoding angiogenic proteins such as vascular endothelial growth factor (VEGF) and nitric oxide synthase (NOS) are of importance for tumor growth and metabolism [6–11].

HIF-1 appeared to be the ideal target for many different anti-angiogenic and anticancer therapies, which boosted the development of small-molecules, which can block the formation of the active HIF-1 complex [12]. However, after Jain's hypothesis about the normalization of tumor vasculature as a strategy for increasing the effectiveness of anticancer drug delivery, it appeared that the opposite approach might be useful in fighting with cancer [13].

HIF-1 activity is controlled by oxygen-dependent regulation of HIF-1α subunit stabilization, through the action of α-ketoglutarate-dependent prolyl hydroxylases (PHD1-3) also known as egg-laying defective nine homolog (EGLN1-3). PHDs, the negative regulators of HIF-1 transcription factor, mark the oxygen-labile α subunit of HIF for proteasomal degradation [14]. Although the major factor regulating PHDs activity is the bioavailability of oxygen, additional factors with a significant role during tumorigenesis may also affect PHDs functioning. It is well

* Corresponding author.
E-mail address: agnieszka.loboda@uj.edu.pl (A. Łoboda).

https://doi.org/10.1016/j.bcp.2020.113922
Received 22 December 2019; Accepted 19 March 2020
Available online 20 March 2020

established that the interactions between HIF-1 and reactive oxygen species (ROS), nitric oxide (NO) and reactive nitrogen species (RNS) may be of great importance, however, they can be exerted in a condition-dependent way. For example, in normoxic conditions, NO prevents, whereas in oxygen deficiency it increases HIF-1 degradation [15,16].

Such interactions may be responsible for the discrepant role of PHDs in tumors. Despite the role in suppressing HIF-1 stabilization, some reports indicated that a decrease in the activity of PHD (especially PHD2) can paradoxically improve the effectiveness of anticancer therapy due to tumor vessel normalization and increased delivery of chemotherapeutics. Mazzone et al. [17] have shown that haplodeficiency of PHD2 in tumor tissue normalized endothelial lining and vessel maturation. This resulted in improved tumor perfusion and oxygenation concomitantly with inhibited tumor cell invasion and metastasis [17]. Other studies pointed out that PHD2 inhibition in breast cancer cells causes a reduction in tumor growth rate [18] and metastasis potential [19]. Therefore, understanding what dictates these differential responses is of great importance for providing more effective cancer therapies.

Both genetic and chemical approaches for PHDs inhibition are available, however, from the clinical point of view, small-molecule inhibitors with oral delivery can be the best option for patient treatment. Of the chemical compounds, the most frequently used are α-ketoglutarate analogues with dimethylallyl glycine (DMOG), applied both *in vitro* and *in vivo*, in mouse [20] and rat models [21]. The limitation of DMOG is its solubility in organic solutions and lack of specificity (as it decreases α-ketoglutarate necessary for other enzymes). Among more specific PHDs inhibitors, molidustat (BAY 85–3934) is considered clinically relevant, due to the good bioavailability when administered as an oral therapy [22] especially for the treatment of anemia associated with chronic diseases [23].

To the best of our knowledge, the effect of molidustat has not been tested in cancer biology yet. Therefore, the aim of this study was to assess the impact of PHDs inhibitor on MDA-MB-231 breast cancer cell viability, clonogenic potential, and sensitization to chemotherapy. We examined also its effectiveness in the xenograft breast cancer model *in vivo*. We show that molidustat exerts anti-tumor properties, which may suggest that targeting of PHDs is a rational approach in monotherapy as well as in the combinational treatment of tumors.

2. Materials and methods

2.1. Cell culture

MDA-MB-231 human breast cancer cell line was obtained from ATCC and cultured under standard conditions (37 °C, 5% CO_2) in low glucose (1.0 g/L) Dulbecco's Modified Eagle's medium - DMEM (Lonza, Basel, Switzerland), supplemented with 10% fetal bovine serum (FBS, Biowest), antibiotics: 100 U/mL penicillin and 100 μg/mL streptomycin (Sigma-Aldrich, St. Louis, MO, USA), 100x non-essential amino acid (NEAA, Gibco, Dublin, Ireland), 100x GlutaMAX (Gibco) and 100 mM sodium pyruvate (Lonza, Basel, Switzerland). For Matrigel angiogenic test, human aortic endothelial cells (HAoEC, passages 8–14, Gibco, Dublin, Ireland) were used. Cells were cultured in Endothelial Cell Growth Medium MV 2 (Lonza, Basel, Switzerland), supplemented with 10% FBS in standard conditions. Cells were routinely screened for mycoplasma contamination using MycoAlert™ Mycoplasma Detection Kit (Lonza, Basel, Switzerland).

2.2. Cells stimulation

Cells were stimulated with 10, 25 and 50 μM molidustat (Ark Pharm, Inc. IL, USA) dissolved in DMSO) for 24, 48 or 72 h. For some experiments, gemcitabine (dissolved in water, 1–10 nM) was used. The control cells received the appropriate solvent. To compare the effect of molidustat with the hypoxic conditions, MDA-MB-231 cells were cultured in hypoxic (0.5% O_2) or atmospheric oxygen conditions (21% O_2).

2.3. MTT viability assay

To assess the viability of cells, MTT (3-(4,5-dimethylthiazol-2-yl)-2,5-diphenyltetrazolium bromide (Sigma-Aldrich, St. Louis, MO, USA) was used. 5,000 cells were seeded in triplicates in 96-well plates and cells were stimulated with molidustat and/or gemcitabine for 48 and 72 h. Then, cells were incubated with 1 mg/mL MTT in a complete medium for 2 h at 37 °C. Formed formazan crystals were dissolved in 100 μL/well of lysis buffer consisting of 0.6% (v/v) acetic acid and 10% (w/v) SDS in DMSO (Chempur, Piekary Śląskie, Poland) and absorbance at 570 nm with the reference at 690 nm was measured using Infinite M200 microplate reader (Tecan, Männedorf, Switzerland). Cells not stained with MTT served as the blank.

2.4. Colony formation assay

1,000 cells were seeded on 6-well plates, stimulated with different concentrations of molidustat and/or gemcitabine and grown for 13 days. Afterwards, cells were fixed with cold (-20 °C), 100% methanol for 20 min on ice and stained with 0.05% (w/v) crystal violet (BioShop Canada Inc, Burlington, ON, Canada) in 20% methanol for 20 min at room temperature. After complete removal of crystal violet and washing with tap water, pictures of the plates were taken using Fusion FX5 XT camera (Vilber, Collégien, France).

2.5. Quantitative real-time PCR

RNA was isolated from cultured cells using Fenozol (A&A Biotechnology, Gdynia, Polska) according to Chomczynski and Sacchi method [24]. RNA concentration and purity were determined using NanoDrop 1000 (Thermo Fisher Scientific, Waltham, MA, USA), and reverse transcription was performed using SuperScript polymerase (Invitrogen, Carlsbad, CA, USA) according to instructions supplied by the manufacturer. Obtained cDNA was used as a template for quantitative real-time PCR with SybrGreen Mix (Sigma-Aldrich, St. Louis, MO, USA) and specific primers recognizing vascular endothelial growth factor A (*VEGF*), *TP53* and *CDKN1* (Table 1). *EEF2* (encoding eukaryotic translation elongation factor 2, EF-2) was used for gene expression normalization. The reaction was performed using StepOnePlus real-time PCR systems (Applied Biosystems, Foster City, CA, USA). Relative transcript abundance was expressed as $2^{-\Delta C_T}$, where ΔC_T is defined as a difference between C_T values obtained for the gene of interest and housekeeping *EEF2* gene.

2.6. Western blot

Cultured cells were lysed with RIPA buffer and 25–50 μg of protein lysates were loaded on 12% SDS-PAGE gel followed by electrophoresis and wet transfer of proteins to nitrocellulose membrane (30 V/overnight). Membranes were blocked with 5% non-fat milk in TBS (Tris-buffered saline, BioShop Canada Inc, Burlington, ON, Canada) + 0.1% (v/v) Tween-20 (BioShop Canada Inc, Burlington, ON, Canada) for 1.5 h at room temperature. Primary antibodies: rabbit anti-HIF-1α (14179S, Cell Signaling Technology, Danvers, MA, USA), mouse anti-p53 (39553,

Table 1
Primers used for qRT-PCR.

Gene	Primer	Sequence
EEF2	forward	5′ – TCAGCACACTGGCATAGAGGC – 3′
	reverse	5′ – GACATCACCAAGGGTGTGCAG – 3′
TP53	forward	5′ – AGTCTAGAGCCACCGTCCAG – 3′
	reverse	5′ – AGTCTGGCTGCCAATCCAGG – 3′
CDKN1	forward	5′ – GCAGACCAGCATGACAGATTT – 3′
	reverse	5′ – GGATTAAGGGCTTCCTCTTGGA – 3′
VEGF	forward	5′ – AAGGAGGAGGGCAGAATCATCACG – 3′
	reverse	5′ – CTCAGTGGGCACACACTCCAG – 3′

Active Motif, Carlsbad, CA, USA), rabbit anti-phospho-p53 (9284S, Cell Signaling Technology, Danvers, MA, USA), rabbit anti-p21 Waf1/Cip1 (2947S, Cell Signaling Technology, Danvers, MA, USA) and mouse anti-α-tubulin (CP06, Calbiochem) diluted 1:1,000 in blocking solution were used for overnight incubation at 4 °C. The next day, membranes were washed and incubated with secondary antibodies conjugated with HRP: goat anti-mouse (BD Pharmingen, San Diego, CA, USA) and goat anti-rabbit (Cell Signaling Technology, Danvers, MA, USA) at dilution of 1:10,000 for 1 h at room temperature. After series of washings, a luminescent substrate for HRP activity (Immobilon Chemiluminescent HRP Substrate, Merck Millipore, Billerica, MA, USA) was added for 10 min and membranes were manually developed on X-ray film.

2.7. Enzyme-linked immunosorbent assay (ELISA)

VEGF released into the cell culture medium from the control and molidustat-treated cells was quantified using Human VEGF ELISA Kit (DY293B, R&D Systems, Minneapolis, MN, Canada) according to the manufacturer's instruction.

2.8. In vitro angiogenesis assay

To assess the influence of molidustat on the angiogenic properties of endothelial cells, conditioned media from MDA-MB-231 cells (collected 24 h and 48 h after stimulation) were used in tube formation assay on Matrigel. 50 μL of the Growth Factor-Reduced Matrigel (BD Biosciences, San Jose, CA, USA) was plated in a 96-well plate and incubated at 37 °C for 30 min. During this time HAoEC cell suspensions were prepared in conditioned media collected from control and molidustat-treated MDA-MB-231 cells. 100 μL of HAoEC cell suspension (10,000 cells) was seeded on the Matrigel for 6 h at 37 °C and endothelial tube formation was analysed using Nikon Eclipse T*i* microscope. The calculation of the number of junctions and the total length of capillaries was performed using ImageJ program.

2.9. Cell cycle analysis

Cells were seeded in a 6-well plate at a density of 1.5×10^5 and after 72 h incubation with different concentrations of molidustat cells were detached and fixed in 4% paraformaldehyde for 10 min at room temperature. For assessment of the effect of hypoxia on MDA-MB-231 cells were cultured in either normoxic or hypoxic conditions for 72 h and thereafter proceeded as above. Then, cells were permeabilized in 0.1% Triton-X100 for 15 min, washed with PBS with 4% FBS and stained with DAPI for 30 min in dark. After subsequent washing with PBS, cells were analyzed using BD LSRFortessa (BD Biosciences, San Jose, CA, USA) flow cytometer with Diva software. Doublets were excluded through gating on DAPI-A versus DAPI-W parameter. Additionally, the DNA histograms were analyzed with ModFit LT software (Verity Software House).

2.10. Flow cytometry analysis of apoptosis

The induction of apoptosis by molidustat was assessed with Hoechst 33342/7-amino-actinomycin D (7-AAD) (BD Biosciences, San Jose, CA, USA) dual staining of the cells and subsequent flow cytometry analysis according to previously published protocols [25]. Apoptotic cells increase uptake of the vital dye Hoechst 33,342 due to the changes in membrane permeability, whereas the nonvital dye 7-AAD distinguishes late apoptotic or necrotic cells that have lost membrane integrity.

2.11. Tumor xenografts

Experiments were carried out in the animal facility of the Jagiellonian University accordingly to the protocols approved by the 2nd Local Institutional Animal Care and Use Committee (IACUC) in Krakow (approval number: 162/2017). NOD/SCID mice (sgNOD.CB-17-Prkdc scid/Rj) were purchased from Janvier Labs (Le Genest-Saint-Isle, France). To test the effect of molidustat on MDA-MB-231 tumor growth, mice were inoculated subcutaneously with 5×10^6 cells in PBS with Matrigel (BD Biosciences, San Jose, CA, USA) (ratio 1:1). After the xenografts reached 100 mm^3, the animals were randomized to receive molidustat (dissolved in methanol:Solutol HS 15:water; 10:20:70, Sigma-Aldrich, St. Louis, MO, USA) or vehicle *via* oral administration (n = 9/group). Molidustat was administered daily for 12 consecutive days at a concentration of 5 mg/kg body weight. The vehicle formulation, the dose, route, and frequency of administration of the inhibitor were based on previously published data [22,26]. Tumor growth and mice weight were measured every 2–3 days. At the end of the experiment tumors and blood were collected for further analysis.

2.12. Total blood cells analysis

Fresh EDTA-anticoagulated blood samples from the control and molidustat-treated mice were analyzed on the Scil Vet ABC hematology analyzer (Gurnee, IL, USA).

2.13. Immunofluorescent detection of blood vessels

For the determination of CD31 and alpha-smooth muscle actin (α-SMA) positive blood vessels, 8 μm thick tumor frozen sections were fixed in cold (-20 °C) acetone (2 min) and 80% methanol (stored at 4 °C) for 5 min according to the protocol described elsewhere [27]. Shortly, after blocking in 10% goat serum + 1% BSA and 0.1% Triton X100 in PBS for 2 h at room temperature, the sections were incubated overnight (at 4 °C) with rat anti-CD31 (BD Pharmingen, San Diego, CA, USA) and rabbit anti-α-SMA (Abcam, Cambridge, UK) primary antibodies diluted 1:200 in blocking solution. Next day, after washing in PBS, the sections were incubated with secondary antibodies: goat anti-rat AlexaFluor 568 (Thermo Fisher Scientific, Waltham, MA, USA) for detection of CD31 (in red) and goat anti-rabbit AlexaFluor 488 (Invitrogen, Carlsbad, CA, USA) for the detection of α-SMA (in green) for 2 h at room temperature in the darkness, washed, counterstained with 10 μg/ml Hoechst 33,342 (Sigma-Aldrich, St. Louis, MO, USA), covered with fluorescence mounting medium (Dako, Carpinteria, CA, USA) and visualized using meta laser scanning confocal microscope (LSM-880; Carl Zeiss, Oberkochen, Germany).

2.14. Statistical analysis

All *in vitro* experiments were performed at least in duplicates and were repeated two or three times. Results are presented as mean ± SD (standard deviation) unless stated otherwise. Statistical analysis was performed in GraphPad Prism Software using t-Student's test or non-parametric Kruskal-Wallis test with Dunn's multiple comparisons post-test. Results were considered statistically significant at $p < 0.05$.

3. Results

3.1. Molidustat stabilizes HIF-1 and increases expression of HIF-1-dependent VEGF, but does not affect the angiogenic potential of endothelial cells

Molidustat is a known PHD inhibitor and HIF-1 regulator [22]. Nonetheless, according to our knowledge, its activity on the MDA-MB-231breast cancer cell line was not tested up to date. Using this cell model we observed stabilization of HIF-1α in the case of the highest (50 μM) concentration of the compound (Fig. 1**A**), however, the expression of VEGF, a known HIF-1-dependent gene, was increased already by 10 μM molidustat after 24 h treatment. Both VEGF mRNA expression and protein release to the media were increased after 24 h and 48 h (Fig. 1 **B, C).** In our hands, this compound enhanced VEGF expression to a similar or even higher level as hypoxia (Fig. 1 **B, C).**

As VEGF is a well-described pro-angiogenic factor, we tested whether the conditioned medium collected from the tumor cells treated

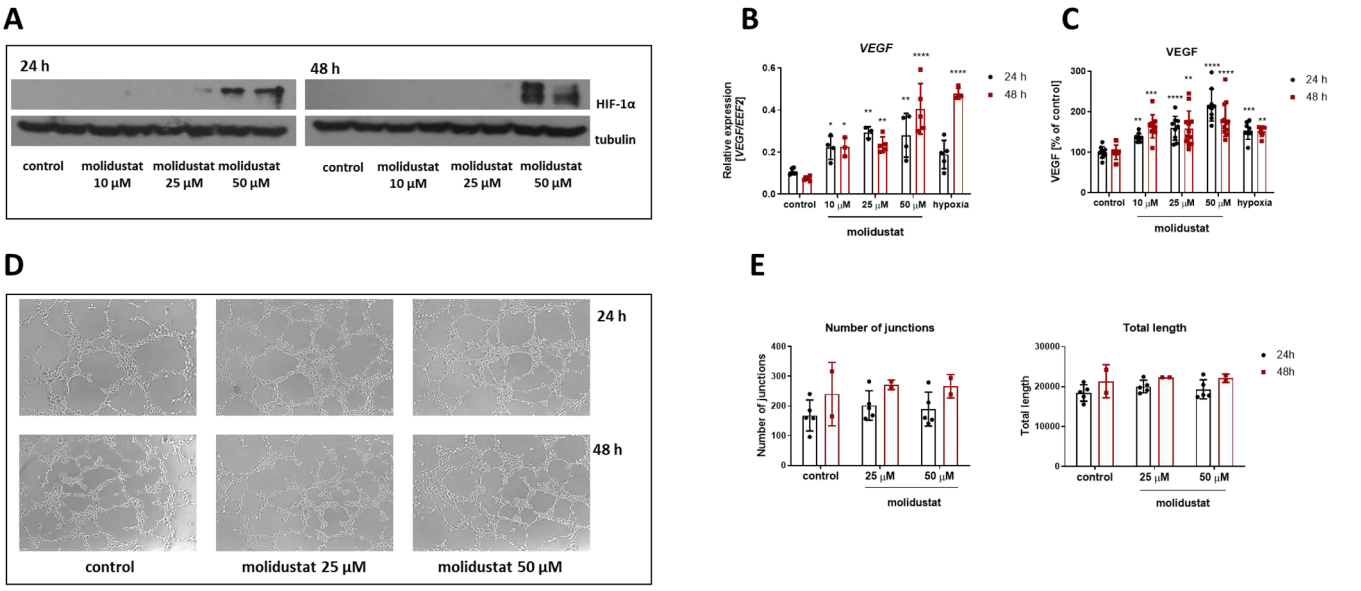

Fig. 1. Molidustat stabilizes HIF-1 and increases the expression of the HIF-1-dependent gene but does not affect the angiogenic potential of endothelial cells. **(A)** Representative western blots showing HIF-1α protein elevation after 24 h and 48 h molidustat treatment at the highest concentration. The expression of VEGF **(B)** mRNA assessed by qRT-PCR and **(C)** protein analyzed by ELISA is potently upregulated after 10–50 μM molidustat stimulation for 24 h and 48 h. A comparable effect was observed after cell culturing in 0.5% O_2. **(D)** Angiogenic test *in vitro* on Matrigel and its quantification **(E)** indicating no difference in angiogenic properties of HAoEC cells cultured in conditioned media from control and molidustat-treated MDA-MB-231 cells. Data are presented as mean ± SD. *p < 0.05; **p < 0.01; ***p < 0.005 (*vs.* control).

with the inhibitor could affect the angiogenic properties of endothelial cells. The capillary formation test on Matrigel of primary human aortal endothelial cells (HAoEC) showed no significant differences when comparing post-treatment media with the inhibitor to the control ones. The observed effects were similar in the media collected after both (24 h and 48 h) timepoints **(**Fig. 1 **D, E).**

3.2. Molidustat decreases viability and clonogenic potential of MDA-MB-231 cells

To check the effect of molidustat on the survival of MDA-MB-231 cells, MTT reduction assay and flow cytometry analysis were performed after treatment of the cells with three concentrations of the inhibitor. There was a dose-dependent decrease in cell viability, which was visible already 48 h after treatment with the lowest concentration of the examined compound (10 μM). The effect was additionally potentiated by the increased time of incubation. At the highest dose (50 μM), a nearly two-fold decrease in cell survival was observed after 72 h as compared to 48 h (Fig. 2**A).** Additionally, the clonogenic potential of MDA-MB-231 cells in response to molidustat was tested. The ability of cells to form colonies was slightly impaired after 10 μM molidustat **(**Fig. 2**B).** However, the number of colonies was greatly diminished in the wells with 25 μM inhibitor added. At the highest concentration, cell survival was dramatically affected to the level, where no colonies could be observed. To check whether molidustat induces cell apoptosis, flow cytometry analysis using double staining with Hoechst/7-AAD was performed. There was an increase in the apoptotic fraction after 72 h of the treatment only at the highest inhibitor concentration in comparison to untreated cells **(**Fig. 2**C).** However, the percentage of apoptotic cells was rather small (up to 8%) pointing at other pathways implemented in the decreased breast cancer cell viability.

3.3. Molidustat sensitizes MDA-MB-231 cells for chemotherapeutic treatment

Although molidustat used as monotherapy, at higher concentrations, affected cell viability and slightly increased apoptosis, we supposed that combined treatment with both HIF-1 inducer and chemotherapeutic drug may enhance the effect on cancer cell viability and self-renewal potential of MDA-MB-231 cells. Indeed, in the breast cancer model, combined treatment with gemcitabine and molidustat exerted a more pronounced effect on cell viability compared to the treatment with PHD inhibitor or chemotherapeutic drug alone (Fig. 3**A**). This effect was even stronger when colony formation potential was assessed. Treatment with molidustat and gemcitabine was very effective, as already 10 μM PHD inhibitor and 2.5 nM gemcitabine led to the almost complete loss of cells self-renewal (Fig. 3**B**)**.** This effect was potentiated at the higher molidustat concentration (25 μM, Fig. 3**C**)**.** Moreover, an increased percentage of the apoptotic fraction of cells treated with both compounds in comparison to gemcitabine-treated cells was evident when flow cytometry analysis was performed **(**Fig. 3**D).**

3.4. Molidustat induces S/G2 cell cycle arrest through activation of p53

As it is well known that cell death in cancer cells can be mediated by p53 activation [28], we checked whether molidustat acts through this signaling pathway in MDA-MB-231 cells. PHD inhibitor treatment did not affect p53 mRNA level, but we found an increase in p53-dependent, cyclin-dependent kinase (CDK) inhibitor p21 (*CDKN1A*, Fig. 4**A**). At the protein level a slight dose-dependent increase in p53 at 72 h timepoint and phosphorylated form of p53 especially at 48 h treatment could be seen (Fig. 4**B**), whereas, there was downregulation of p21 protein level, which is known to be implicated in cell growth arrest. Keeping in mind that p53 activation contributes to growth arrest not only through p21, we checked the molidustat effect on MDA-MB-231 cell cycle progression. The results showed an increased S-G2/M cell cycle arrest in MDA-MB-231 cells treated with 50 μM molidustat **(**Fig. 4**C, D)**. A comparable effect was noted when breast cancer cells were subjected to conditions of low oxygen concentration **(**Fig. 4**D).**

3.5. Molidustat reduces the growth of MDA-MB-231 in vivo

To expand our *in vitro* observations, we performed an *in vivo* study to evaluate the effectiveness of molidustat on tumor growth**.** For this

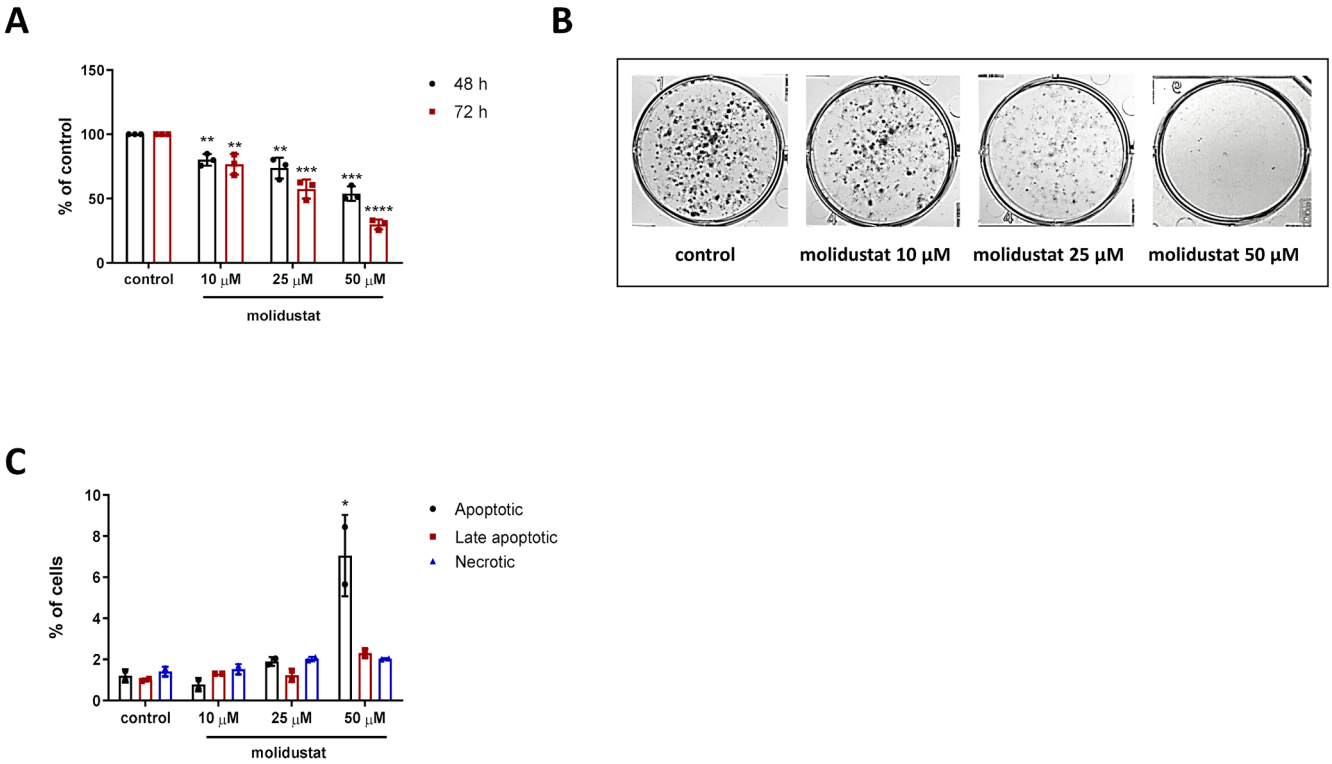

Fig. 2. HIF-1 stabilizator decreases viability as well as the clonogenic potential of MDA-MB-231 cells. **(A)** Molidustat decreases MDA-MB-231 cell viability. Cells were incubated with increasing doses of molidustat for 48 h − 72 h. Thereafter, cell viability was assessed using MTT assay. **(B)** HIF-1 activation with molidustat impairs the clonogenic potential of MDA-MB-231 cells. Cells were grown in the presence or absence of molidustat (10–50 μM) for 13 days. Exemplary photographs of plates/colonies are shown. **(C)** Molidustat caused a slight increase in apoptosis in the MDA-MB-231 cell line only at 50 μM, as assessed through flow cytometry analysis. Data are presented as mean ± SD. *p < 0.05; **p < 0.01; ***p < 0.005; ****p < 0.001 (*vs.* control).

purpose, mice were subcutaneously inoculated with MDA-MB-231 cells and xenograft-bearing animals with tumor volumes exceeding 100 mm^3 received 5 mg/kg body weight molidustat daily for the consecutive 12 days. Accordingly to the *in vitro* experiments, molidustat decreased breast tumor growth compared to the control group receiving vehicle (Fig. 5**A**). To check if the decreased tumor growth is connected with changes in vascularization, CD31/α-SMA staining was performed on frozen tumor sections. We did not observe differences in CD31/ α-SMA positive blood abundance (Fig. 5**B**), similarly to *in vitro* angiogenic assay on Matrigel (Fig. 1**D, E**). Molidustat treatment did not cause any changes in the body weight of the tested animals (Fig. 5**C**) but pronounced changes in blood cell count were found. There was an increase in the hematocrit (HCT), hemoglobin (HGB), red blood cells (RBC) count, whereas a decrease in platelets (PLT) number could be observed (Fig. 5**D**). Molidustat treatment in mice caused a decrease in the percentage of the monocytes and granulocytes at the expense of lymphocytes (Fig. 5**D**). Summarizing, our results show that molidustat treatment causes a reduction of breast cancer tumors in xenograft-bearing mice, without influencing tumor vascularization.

4. Discussion

Hypoxia is a common feature of malignant tumors and it may interplay with tumor chemoresistance, radioresistance, invasiveness, and angiogenesis. Although the role of HIF-1 in the development of solid tumors is well established, some studies demonstrated also that this factor can exhibit either tumor-promoting or tumor-suppressing properties in a context-dependent manner. Moreover, as HIF-1 activity is dependent on PHDs enzymes, it was suggested that therapeutic targeting of the PHDs family could be a rational approach in the anti-tumor treatment.

Cobalt chloride, DMOG, and deferoxamine are, among others, the possible HIF-1 inducers tested already in various *in vitro* and *in vivo* settings. Nonetheless, another compound, namely molidustat, is characterized by greater specificity and well-tolerated oral delivery, features that are extremely beneficial in the context of therapeutic applications [22,23]. Therefore, we investigated the possible protective effect of HIF-1 stabilization in the MDA-MB-231 breast cancer cell line. We found that molidustat, reported to stimulate erythropoiesis and used for anemia treatment [22,23], may decrease tumor cell viability and self-renewal capacity of breast cancer cells together with enhanced effectiveness of the chemotherapeutic drug, gemcitabine. We confirmed our *in vitro* results in a xenograft model, by showing decreased tumor volume after oral administration of PHDs inhibitor. Intriguingly, the mechanism of molidustat action is not related to angiogenesis, but it may rely on p53 activation and subsequent cell cycle arrest. We believe that with this data, we add a further piece to the understanding of the HIF1-regulation based anticancer therapies.

Our results indicate a dose-dependent increase in MDA-MB-231 cell mortality, as well as a slight increase in the apoptotic cell fraction after the highest concentration of molidustat. Additionally, we have shown a similar effect of low oxygen concentration on MDA-MB-231 cell cycle arrest, suggesting that HIF stabilization by molidustat and culturing of the cells under hypoxic conditions trigger the same mechanism. Importantly, the results were reproduced also *in vivo* through the observation of hampered tumor growth in the xenograft model. It was previously shown that HIF-1α is involved in hypoxia-induced apoptosis via the stabilization of the p53 tumor suppressor gene [29]. In the current study molidustat treatment of MDA-MB-231 cells *in vitro* caused a slight increase, as well as phosphorylation of p53 protein, especially after a longer incubation time. Concomitantly, the p53 stabilization in this breast cancer cell line was associated with the increase of *CDKN1A*, one of the validated p53 target genes [30]. This was accompanied by S/G2 cell cycle arrest, downregulation of p21 protein levels and a slight increase in apoptosis. Such an effect of molidustat is comparable to naphthalene diimide derivates, which

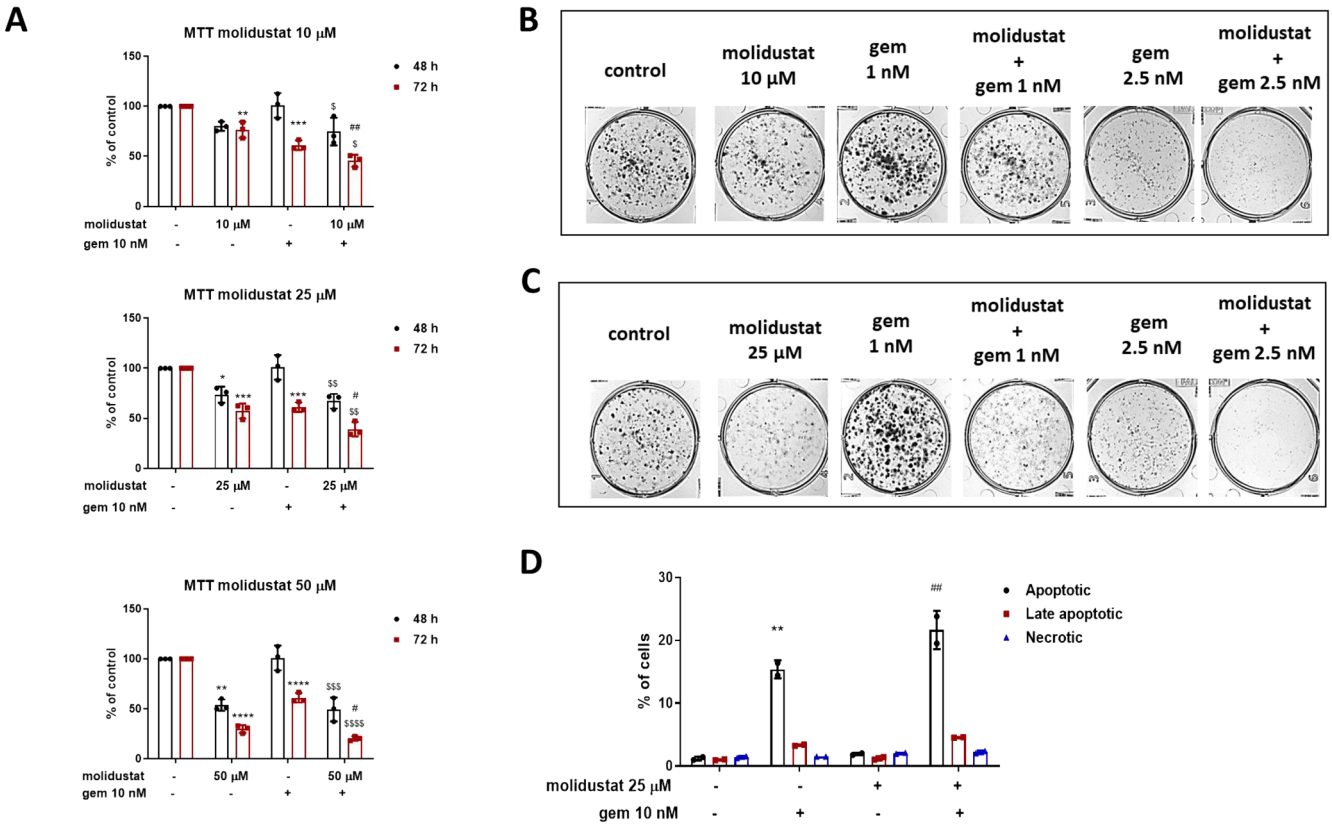

Fig. 3. Molidustat sensitizes MDA-MB-231 cells for chemotherapeutic treatment. Viability assessed by MTT **(A)** and clonogenic potential **(B, C)** of MDA-MB-231 cells after co-treatment with various concentrations of molidustat and gemcitabine. Representative photographs of colony formation assay after 13 days of treatment with 10 μM **(B)** and 25 μM **(C)** molidustat and different concentrations of gemcitabine. **(D)** Flow cytometry analysis of apoptotic cells. Data are presented as mean ± SD. $^{*}p < 0.05$; $^{**}p < 0.01$; $^{***}p < 0.005$; $^{****}p < 0.001$ (*vs.* control); $^{\$}p < 0.05$; $^{\$\$}p < 0.01$; $^{\$\$\$}p < 0.005$; $^{\$\$\$\$}p < 0.001$ (*vs.* gemcitabine alone-treated cells); $^{\#}p < 0.05$; $^{\#\#}p < 0.01$ (*vs.* molidustat alone-treated cells).

anticancer properties were shown to be dependent on downregulation of p21 and S phase cell cycle arrest [31]. Even though p21 is considered as the main mediator of cell cycle arrest, p53 activation can result in G2/M arrest through repression of *CDC25C* promotor or induction of miR-34a [28]. It was shown that MDA-MB-231 cells carry a single *TP53* allele with a mutation at codon 280 (exon 8, AGA [Arg] > AAA [Lys]; R280K) with known gain-of-function implemented in invasion, migration, and formation of metastasis [32]. Great variability in p53 binding site sequence, affinity, conformation and relative location to the proximal promoter is evident, as some tumor-derived p53 mutants fail to bind and/or activate pro-apoptotic genes, but still retain the ability to activate the p21 promoter, thereby revealing different constraints for p53 binding and transactivation [33]. Therefore, current findings on the molidustat effect on the cell cycle arrest in this p53-mutated cell line, together with strongly decreased clonogenic potential and cell survival could have an important translation for therapeutic strategies in p53-mutated cancers.

Induction of angiogenesis through local sprouting and neovascularization is essential for the rapid growth of solid tumors. HIF-1 activation leads to accelerated angiogenesis through e.g. VEGF-dependent mechanisms, however, other factors may greatly contribute to this process. It could be expected that reduced PHDs level together with HIF-1 stabilization would stimulate neovascularization. Nevertheless, the CD31/α-SMA staining from the current *in vivo* study revealed that tumor vessel abundance and structure were comparable between control and molidustat-treated animals. In our hands, the level of VEGF increased potently after molidustat treatment, however, tumor angiogenesis *in vitro* and *in vivo* was not much affected suggesting that other (anti-angiogenic) factors may be involved in the observed mechanisms. Several PHDs-regulated molecules have been identified, including IL-8, as the factors contributing to the tumor-inducing effects in stably transfected PHD2 knockdown tumor model [34]. Quite importantly, when heterozygous deficiency of PHD2 was created by Mazzone et al., no alterations in tumor vessel density or lumen size have been observed [17]. However, the differences in endothelial cells shape and phenotype, resulting in the normalization of endothelial lining was evident. This was accompanied by improved tumor perfusion and oxygenation what may be important when chemotherapy treatment is considered. Importantly, our *in vitro* studies revealed that molidustat increases the sensitivity of MDA-MB-231 to gemcitabine treatment. However, the exact mechanism responsible for this phenomenon has to be studied in more detail.

Our xenograft experiment revealed the tumor inhibitory effect of molidustat *in vivo*. This response is consistent with the observations reported by Wottawa et al., [18], who found that genetic inhibition of PHD2 with specific shRNAs decreased tumor-forming potential of MDA-MB-231 cells in a SCID mouse model. In our hands, the limited cloning potential of MDA-MB-231 cells after molidustat treatment was evident. All above, together with cell cycle alterations, suggests that increased cellular mortality and severe proliferative arrest are the major mechanisms of molidustat-mediated toxicity.

In conclusion, although it is generally accepted that tumor hypoxia and HIF-1 activation correlates with unfavorable disease outcome, malignancy and resistance to therapy, here we have shown that molidustat, PHDs inhibitor and HIF-1 stabilizator, may exert anticancer effects toward breast cancer cells *in vitro* and *in vivo*, but does not affect angiogenesis.

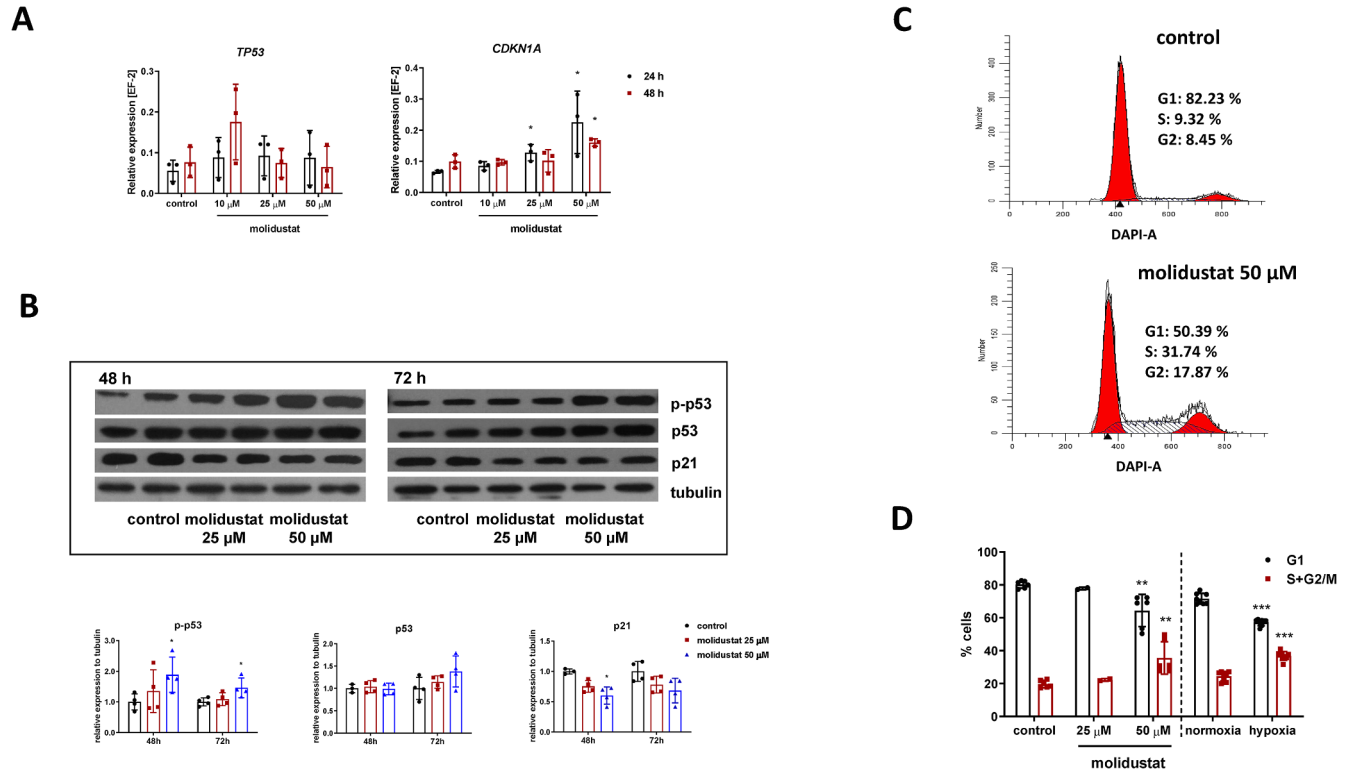

Fig. 4. HIF-1 stabilizator induces S/G2 cell cycle arrest through activation of p53. **(A)** *TP53* and *CDKN1A* expression assessed by qRT-PCR; **(B)** protein level of total and phosphorylated p53 together with p21 checked by Western blotting together with densitometric analysis; **(C)** Representative histograms and **(D)** quantification of cell cycle analysis of MDA-MB-231 after 72 h of molidustat treatment. Additionally, cell cycle analysis was performed on cells cultured in normoxic (21% O_2) and hypoxic (0.5% O_2) conditions. The statistical significance is calculated to the respective control. Data are presented as mean ± SD. *p < 0.05; **p < 0.01 (*vs.* control).

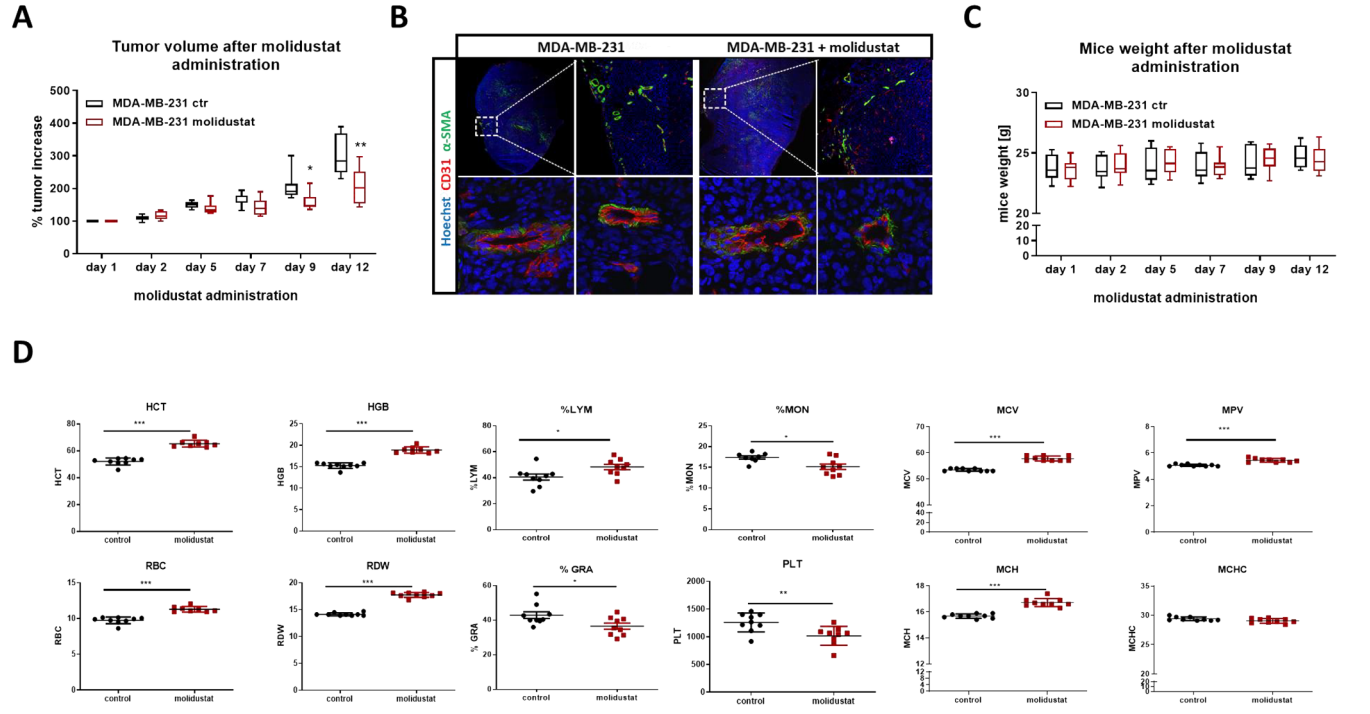

Fig. 5. Molidustat hampers the growth of MDA-MB-231 *in vivo*. **(A)** Xenograft growth kinetics in mice inoculated with MDA-MB-231 cells and treated with molidustat or vehicle. Data are presented as min to max values; **(B)** Representative immunofluorescent staining of CD31/α-SMA positive vessels in tumors from control and molidustat-treated animals. **(C)** Total body weight was measured during the experiment. Data are presented as min to max values and statistical analysis was performed with multiple t-tests; **(D)** The changes in blood cell count after molidustat treatment after the measurement on the hematology analyzer. n = 9 mice/group; *p < 0.05; **p < 0.01; ***p < 0.005 (*vs.* control).

CRediT authorship contribution statement

Neli Kachamakova-Trojanowska: Conceptualization, Methodology, Investigation, Formal analysis, Writing - original draft, Writing - review & editing, Visualization. **Paulina Podkalicka:** Investigation, Visualization. **Tomasz Bogacz:** Investigation, Visualization. **Szymon Barwacz:** Investigation, Visualization. **Alicja Józkowicz:** Conceptualization, Supervision. **Józef Dulak:** Conceptualization, Supervision, Writing - review & editing, Project administration, Funding acquisition. **Agnieszka Łoboda:** Conceptualization, Methodology, Investigation, Formal analysis, Writing - original draft, Writing - review & editing, Visualization, Supervision.

Declaration of Competing Interest

The authors declare that they have no known competing financial interests or personal relationships that could have appeared to influence the work reported in this paper.

Acknowledgements

This work was supported by the National Centre for Research and Development grant STRATEGMED1/233574/15/NCBR/2015. We thank the staff from the animal facility of the Faculty of Biochemistry, Biophysics and Biotechnology for their excellent technical assistance.

References

[1] C.M. Perou, T. Sørlie, M.B. Eisen, M. van de Rijn, S.S. Jeffrey, C.A. Rees, J.R. Pollack, D.T. Ross, H. Johnsen, L.A. Akslen, O. Fluge, A. Pergamenschikov, C. Williams, S.X. Zhu, P.E. Lønning, A.L. Børresen-Dale, P.O. Brown, D. Botstein, Molecular portraits of human breast tumours, Nature 406 (2000) 747–752, https://doi.org/10.1038/35021093.

[2] C. Curtis, S.P. Shah, S.-F. Chin, G. Turashvili, O.M. Rueda, M.J. Dunning, D. Speed, A.G. Lynch, S. Samarajiwa, Y. Yuan, S. Gräf, G. Ha, G. Haffari, A. Bashashati, R. Russell, S. McKinney, METABRIC Group, A. Langerød, A. Green, E. Provenzano, G. Wishart, S. Pinder, P. Watson, F. Markowetz, L. Murphy, I. Ellis, A. Purushotham, A.-L. Børresen-Dale, J.D. Brenton, S. Tavaré, C. Caldas, S. Aparicio, The genomic and transcriptomic architecture of 2,000 breast tumours reveals novel subgroups, Nature 486 (2012) 346–352, https://doi.org/10.1038/nature10983.

[3] A. Marusyk, V. Almendro, K. Polyak, Intra-tumour heterogeneity: a looking glass for cancer? Nat. Rev. Cancer 12 (2012) 323–334, https://doi.org/10.1038/nrc3261.

[4] A. Loboda, A. Jozkowicz, J. Dulak, HIF-1 versus HIF-2–is one more important than the other? Vasc.Pharmacol. 56 (2012) 245–251, https://doi.org/10.1016/j.vph.2012.02.006.

[5] D.M. Gilkes, G.L. Semenza, Role of hypoxia-inducible factors in breast cancer metastasis, Future Oncol. Lond. Engl. 9 (2013) 1623–1636, https://doi.org/10.2217/fon.13.92.

[6] H. Zhong, F. Agani, A.A. Baccala, E. Laughner, N. Rioseco-Camacho, W.B. Isaacs, J.W. Simons, G.L. Semenza, Increased expression of hypoxia inducible factor-1alpha in rat and human prostate cancer, Cancer Res. 58 (1998) 5280–5284.

[7] H. Zhong, A.M. De Marzo, E. Laughner, M. Lim, D.A. Hilton, D. Zagzag, P. Buechler, W.B. Isaacs, G.L. Semenza, J.W. Simons, Overexpression of hypoxia-inducible factor 1alpha in common human cancers and their metastases, Cancer Res. 59 (1999) 5830–5835.

[8] K.L. Talks, H. Turley, K.C. Gatter, P.H. Maxwell, C.W. Pugh, P.J. Ratcliffe, A.L. Harris, The expression and distribution of the hypoxia-inducible factors HIF-1alpha and HIF-2alpha in normal human tissues, cancers, and tumor-associated macrophages, Am. J. Pathol. 157 (2000) 411–421, https://doi.org/10.1016/s0002-9440(10)64554-3.

[9] A. Giatromanolaki, E. Sivridis, C. Kouskoukis, K.C. Gatter, A.L. Harris, M.I. Koukourakis, Hypoxia-inducible factors 1alpha and 2alpha are related to vascular endothelial growth factor expression and a poorer prognosis in nodular malignant melanomas of the skin, Melanoma Res. 13 (2003) 493–501, https://doi.org/10.1097/01.cmr.0000056268.56735.4c.

[10] S.C. Hanna, B. Krishnan, S.T. Bailey, S.J. Moschos, P.-F. Kuan, T. Shimamura, L.D. Osborne, M.B. Siegel, L.M. Duncan, E.T. O'Brien, R. Superfine, C.R. Miller, M.C. Simon, K.-K. Wong, W.Y. Kim, HIF1α and HIF2α independently activate SRC to promote melanoma metastases, J. Clin. Invest. 123 (2013) 2078–2093, https://doi.org/10.1172/JCI66715.

[11] G.N. Masoud, W. Li, HIF-1α pathway: role, regulation and intervention for cancer therapy, Acta Pharm. Sin. B. 5 (2015) 378–389, https://doi.org/10.1016/j.apsb.2015.05.007.

[12] J. Li, W. Xi, X. Li, H. Sun, Y. Li, Advances in inhibition of protein-protein interactions targeting hypoxia-inducible factor-1 for cancer therapy, Bioorg. Med. Chem. 27 (2019) 1145–1158, https://doi.org/10.1016/j.bmc.2019.01.042.

[13] R.K. Jain, Normalizing tumor vasculature with anti-angiogenic therapy: a new paradigm for combination therapy, Nat. Med. 7 (2001) 987–989, https://doi.org/10.1038/nm0901-987.

[14] A.M. Meneses, B. Wielockx, PHD2: from hypoxia regulation to disease progression, Hypoxia. 4 (2016) 53–67, https://doi.org/10.2147/HP.S53576.

[15] U. Berchner-Pfannschmidt, H. Yamac, B. Trinidad, J. Fandrey, Nitric oxide modulates oxygen sensing by hypoxia-inducible factor 1-dependent induction of prolyl hydroxylase 2, J. Biol. Chem. 282 (2007) 1788–1796, https://doi.org/10.1074/jbc.M607065200.

[16] E. Metzen, J. Zhou, W. Jelkmann, J. Fandrey, B. Brüne, Nitric oxide impairs normoxic degradation of HIF-1alpha by inhibition of prolyl hydroxylases, Mol. Biol. Cell 14 (2003) 3470–3481, https://doi.org/10.1091/mbc.e02-12-0791.

[17] M. Mazzone, D. Dettori, R.L. de Oliveira, S. Loges, T. Schmidt, B. Jonckx, Y.-M. Tian, A.A. Lanahan, P. Pollard, C.R. de Almodovar, F. De Smet, S. Vinckier, J. Aragonés, K. Debackere, A. Luttun, S. Wyns, B. Jordan, A. Pisacane, B. Gallez, M.G. Lampugnani, E. Dejana, M. Simons, P. Ratcliffe, P. Maxwell, P. Carmeliet, Heterozygous deficiency of PHD2 restores tumor oxygenation and inhibits metastasis via endothelial normalization, Cell 136 (2009) 839–851, https://doi.org/10.1016/j.cell.2009.01.020.

[18] M. Wottawa, P. Leisering, M. von Ahlen, M. Schnelle, S. Vogel, C. Malz, M.R. Bordoli, G. Camenisch, A. Hesse, J. Napp, F. Alves, G. Kristiansen, K. Farhat, D.M. Katschinski, Knockdown of prolyl-4-hydroxylase domain 2 inhibits tumor growth of human breast cancer MDA-MB-231 cells by affecting TGF-β1 processing, Int. J. Cancer 132 (2013) 2787–2798, https://doi.org/10.1002/ijc.27982.

[19] C.D. Madsen, J.T. Pedersen, F.A. Venning, L.B. Singh, E. Moeendarbary, G. Charras, T.R. Cox, E. Sahai, J.T. Erler, Hypoxia and loss of PHD2 inactivate stromal fibroblasts to decrease tumour stiffness and metastasis, EMBO Rep. 16 (2015) 1394–1408 https://doi.org/10.15252/embr.201540107.

[20] S. Koyama, S. Matsunaga, M. Imanishi, Y. Maekawa, H. Kitano, H. Takeuchi, S. Tomita, Tumour blood vessel normalisation by prolyl hydroxylase inhibitor repaired sensitivity to chemotherapy in a tumour mouse model, Sci. Rep. 7 (2017) 45621, https://doi.org/10.1038/srep45621.

[21] Q. Yuan, O. Bleiziffer, A.M. Boos, J. Sun, A. Brandl, J.P. Beier, A. Arkudas, M. Schmitz, U. Kneser, R.E. Horch, PHDs inhibitor DMOG promotes the vascularization process in the AV loop by HIF-1a up-regulation and the preliminary discussion on its kinetics in rat, BMC Biotech. 14 (2014) 112, https://doi.org/10.1186/s12896-014-0112-x.

[22] I. Flamme, F. Oehme, P. Ellinghaus, M. Jeske, J. Keldenich, U. Thuss, Mimicking hypoxia to treat anemia: HIF-stabilizer BAY 85–3934 (Molidustat) stimulates erythropoietin production without hypertensive effects, PLoS ONE 9 (2014) e111838, , https://doi.org/10.1371/journal.pone.0111838.

[23] A.A. Joharapurkar, V.B. Pandya, V.J. Patel, R.C. Desai, M.R. Jain, Prolyl Hydroxylase Inhibitors: A Breakthrough in the Therapy of Anemia Associated with Chronic Diseases, J. Med. Chem. 61 (2018) 6964–6982, https://doi.org/10.1021/acs.jmedchem.7b01686.

[24] P. Chomczynski, N. Sacchi, Single-step method of RNA isolation by acid guanidinium thiocyanate-phenol-chloroform extraction, Anal. Biochem. 162 (1987) 156–159, https://doi.org/10.1006/abio.1987.9999.

[25] I. Schmid, C. Uittenbogaart, B.D. Jamieson, Live-cell assay for detection of apoptosis by dual-laser flow cytometry using Hoechst 33342 and 7-amino-actinomycin D, Nat. Protoc. 2 (2007) 187–190, https://doi.org/10.1038/nprot.2006.458.

[26] H. Beck, M. Jeske, K. Thede, F. Stoll, I. Flamme, M. Akbaba, J.-K. Ergüden, G. Karig, J. Keldenich, F. Oehme, H.-C. Militzer, I.V. Hartung, U. Thuss, Discovery of Molidustat (BAY 85-3934): A Small-Molecule Oral HIF-Prolyl Hydroxylase (HIF-PH) Inhibitor for the Treatment of Renal Anemia, ChemMedChem 13 (2018) 988–1003, https://doi.org/10.1002/cmdc.201700783.

[27] B. Krist, P. Podkalicka, O. Mucha, M. Mendel, A. Sępioł, O.M. Rusiecka, E. Józefczuk, K. Bukowska-Strakova, A. Grochot-Przęczek, M. Tomczyk, D. Klóska, M. Giacca, P. Maga, R. Niżankowski, A. Józkowicz, A. Łoboda, J. Dulak, U. Florczyk-Soluch, miR-378a influences vascularization in skeletal muscles, Cardiovasc. Res. (2019), https://doi.org/10.1093/cvr/cvz236.

[28] J. Chen, The Cell-Cycle Arrest and Apoptotic Functions of p53 in Tumor Initiation and Progression, Cold Spring Harb. Perspect. Med. 6 (2016) a026104, , https://doi.org/10.1101/cshperspect.a026104.

[29] A.E. Greijer, E. van der Wall, The role of hypoxia inducible factor 1 (HIF-1) in hypoxia induced apoptosis, J. Clin. Pathol. 57 (2004) 1009–1014, https://doi.org/10.1136/jcp.2003.015032.

[30] M. Fischer, Census and evaluation of p53 target genes, Oncogene 36 (2017) 3943–3956, https://doi.org/10.1038/onc.2016.502.

[31] S.K. Gurung, S. Dana, K. Mandal, P. Mukhopadhyay, N. Mondal, Downregulation of c-Myc and p21 expression and induction of S phase arrest by naphthalene diimide derivative in gastric adenocarcinoma cells, Chem. Biol. Interact. 304 (2019) 106–123, https://doi.org/10.1016/j.cbi.2019.02.010.

[32] P.A.J. Muller, K.H. Vousden, Mutant p53 in cancer: new functions and therapeutic opportunities, Cancer Cell 25 (2014) 304–317, https://doi.org/10.1016/j.ccr.2014.01.021.

[33] J.M. Espinosa, R.E. Verdun, B.M. Emerson, p53 Functions through Stress- and Promoter-Specific Recruitment of Transcription Initiation Components before and after DNA Damage, Mol. Cell 12 (2003) 1015–1027, https://doi.org/10.1016/S1097-2765(03)00359-9.

[34] D.A. Chan, T.L.A. Kawahara, P.D. Sutphin, H.Y. Chang, J.-T. Chi, A.J. Giaccia, Tumor vasculature is regulated by PHD2-mediated angiogenesis and bone marrow-derived cell recruitment, Cancer Cell 15 (2009) 527–538, https://doi.org/10.1016/j.ccr.2009.04.010.